Causality study and numerical response of the magnetic permeability as a function of the frequency of ferrites using Kramers–Kronig relations

Walter G. Fano[a,b,*], Silvina Boggi[a], Adrián C. Razzitte[a]

[a] *Facultad de Ingeniería, Universidad de Buenos Aires, Paseo Colón 850, C1063EHA Buenos Aires, Argentina*

[b] *Instituto Tecnológico de Buenos Aires, Av. Eduardo Madero 399, C11106ACD Buenos Aires, Argentina*

Abstract

In this paper, the numerical treatment of magnetic loss of NiZn, MnZn, Ni_2Y, and NiZnCu ferrite and their composites, by using Krameres–Kronig relations, is investigated. The complex magnetic permeability spectra for ferromagnetic materials have been studied. Due to the principle of causality and time independence in the relation between magnetic induction B and magnetic field H, the real and the imaginary part of the complex magnetic permeability are mutually dependent, and the correlation is given by the Krameres–Kronig equations. Through them, it is possible to measure the real component of the complex magnetic permeability, assuming the real component is given, and by the Hilbert transform, the imaginary part of the magnetic permeability can be calculated. Magnetic circuit model has been studied theoretically, focusing on the model's poles in the complex plane to verify the principle of causality and the temporary independence.

Keywords: Magnetic permeability; Ferrites; NiZn; MnZn; Magnetic properties; Kramers–Kronig; Hilbert

1. Introduction

The electromagnetic theory can be used to describe the macroscopic properties of matter, these electromagnetic fields may be characterized by four vectors: electric field **E**, magnetic flux density **B**, electric flux density **D**, and magnetic field **H**, which at ordinary points satisfy Maxwell's equations [1].

If the physical properties of the sample can be considered linear, homogeneous, and isotropic, the relation between vectors **B** and **H** are called magnetic permeability μ:

$$\mathbf{B} = \mu\mathbf{H}. \tag{1}$$

Also, an important parameter in magnetic materials is the magnetic susceptibility χ, which relates the magnetization vector **M** with the magnetic field vector **H**:

$$\mathbf{M} = \chi\mathbf{H}. \tag{2}$$

*Corresponding author. Instituto Tecnológico de Buenos Aires, Av. Eduardo Madero 399, C11106ACD Buenos Aires, Argentina. Tel.: +54 11 6393 4800.

E-mail address: gustavo.fano@ieee.org (W.G. Fano).

Magnetic permeability μ and magnetic susceptibility χ are also related to each other by [1]

$$\mu = 1 + \chi. \tag{3}$$

Actually, magnetic materials in sinusoidal fields have magnetic losses and these can be expressed taking μ and χ as complex parameters [2]:

$$\mu = \mu' + j\mu'', \tag{4}$$

$$\chi = \chi' + j\chi''. \tag{5}$$

The magnetic permeability μ' and the loss factor μ'' of the magnetic materials are relevant factors to design devices like inductors, transformers, and wave absorbers for microwaves, among others. Therefore, it is advisable to investigate the behavior of the magnetic materials as a function of the frequency [3,4].

In the frequency range from RF to microwaves, the permeability spectra of ferrite material can be characterized by the different magnetizing mechanisms, domain-wall motion and gyromagnetic spin rotation [11–13].

So, magnetic susceptibility χ can be expressed as the contribution of two terms, gyromagnetic spin (χ_s), and domain wall (χ_d) [5,6]:

$$\chi = \chi_d + \chi_s, \tag{6}$$

$$\mu_r = 1 + \chi_d + \chi_s. \tag{7}$$

Domain wall process can be studied with an equation of motion in which the pressure ($k-H$) is equated to the sum of the three terms:

$$m_e \frac{d^2 z}{dt} + \beta \frac{dz}{dt} + \delta z = kH, \tag{8}$$

where m_e is the effective mass, β is the damping factor, and δ the elasticity factor, while k is a proportionality factor.

The relation between z, the spatial coordinate, and the magnetic dipolar moment is $m = pz$, where p is the intensity of magnetic pole, and $M = Nm$, where N is the number of particles [7,8].

Assuming that the magnetic field has harmonic excitation, the full solution of the above equation of motion gives the characteristic behavior of susceptibility [8]:

$$\chi_d = \frac{\omega_d^2 \chi_{d0}}{\omega_d^2 - \omega^2 - j\omega\beta}, \tag{9}$$

where ω_d is the resonance frequency of domain-wall ($\omega_d^2 = \delta/m$) and χ_{d0} is the static magnetic susceptibility ($\chi_{d0} = k-p/\delta$).

Gyromagnetic spin contribution can be studied with a magnetodynamic equation [3]:

$$\frac{d\mathbf{M}}{dt} = \gamma_e(\mathbf{M} \times \mathbf{H}) + \frac{\alpha}{M}\mathbf{M} \times \frac{d\mathbf{M}}{dt}, \tag{10}$$

where γ_e is the gyromagnetic ratio and α is the damping factor.

Assuming that the magnetic field and the magnetization are harmonic functions:

$$H = H_i + h e^{+j\omega t},$$

$$M = M_0 + m e^{+j\omega t},$$

where H_i is the total internal field and M_0 is the saturated magnetization of the ferrite.

Then the magnetic susceptibility χ_s can be expressed as

$$\chi_s = \frac{(\omega_s + j\omega\alpha)\omega_s \chi_{s0}}{(\omega_s^2 + j\omega\alpha)^2 - \omega^2}, \tag{11}$$

where $\omega_s = -\gamma H_i$ (the resonance frequency of the spin component) and $\chi_{s0} = -\gamma M_0$ (the static magnetic susceptibility).

Thus, the total magnetic permeability results (see Greiner Ref. [8]):

$$\mu = 1 + \frac{\omega_d^2 \chi_{d0}}{\omega_d^2 - \omega^2 - j\omega\beta} + \frac{(\omega_s + j\omega\alpha)\omega_s \chi_{s0}}{(\omega_s^2 + j\omega\alpha)^2 - \omega^2}. \tag{12}$$

The real and imaginary parts of formula (12) can be derived as follows:

$$\mu'(\omega) = 1 + \frac{\omega_d^2 \chi_{d0}(\omega_d^2 - \omega^2)}{(\omega_d^2 - \omega^2)^2 + \omega^2\beta^2} + \frac{\omega_s^2 \chi_{s0}(\omega_s^2 - \omega^2) + \omega^2\alpha^2}{(\omega_s^2 - \omega^2(1+\alpha^2))^2 + 4\omega^2\omega_s^2\alpha^2}, \tag{13}$$

$$\mu''(\omega) = \frac{\omega_d^2 \chi_{d0}\omega\beta}{(\omega_d^2 - \omega^2)^2 + \omega^2\beta^2} + \frac{\omega_s \chi_{s0}\omega\alpha(\omega_s^2 + \omega^2(1+\alpha^2))}{(\omega_s^2 - \omega^2(1+\alpha^2))^2 + 4\omega^2\omega_s^2\alpha^2}. \tag{14}$$

According to the principle of causality, the values of **B** at a certain moment can only be dependent of the **H** values, which occurred previously. Therefore, there is a direct relation between μ' and μ'', this relation is given by the Kramers–Kronig relation [10,16]

$$\mu'_r(\omega) - \mu_{r1} = \frac{1}{\pi} P \int_{-\infty}^{+\infty} \frac{\mu''_r(x')\,dx}{x - \omega}, \tag{15}$$

$$\mu''_r(\omega) = -\frac{1}{\pi} P \int_{-\infty}^{+\infty} \frac{(\mu'_r(x') - \mu_{r1})\,dx}{x - \omega}, \tag{16}$$

where $\mu_{r1} = \mu'(\omega_{max})$ is the real part of the relative magnetic permeability for the maximum frequency.

The relationship between μ' and μ'' shows that the mechanisms of energy storage and energy dissipation are two aspects of the same phenomenon. Hence, if one of the terms is known, even only approximately (for instance, by an experimental way), the other can be deduced. The losses, represented by the imaginary part of the magnetic permeability, can be extremely small; however, they are always present [10].

The well-known Kramers–Kronig relations were obtained taking a complex integration along curve C that is shown in Fig. 1, according to the Cauchy Theorem [9]:

$$\oint_C \frac{\mu_r(\omega) - \mu_{r1}}{\omega - \omega_0}\,d\omega = 0. \tag{17}$$

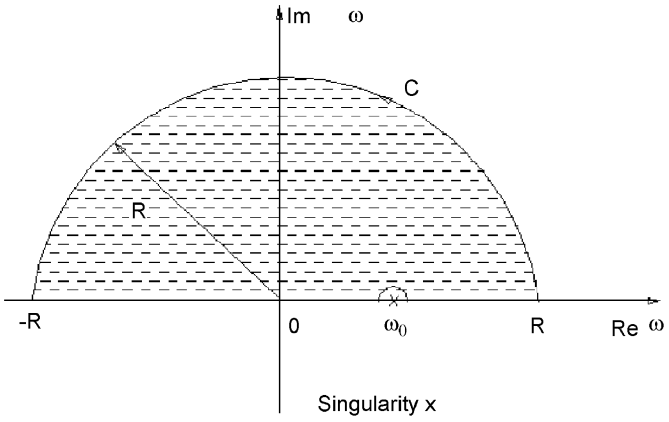

Fig. 1. Integration path used in Eq. (12).

Table 1
Permeability dispersion parameters of sintered Mn–Zn and Ni–Zn ferrite reported by Tsutaoka [6]

	Density (g/cm^3)	Domain-wall component			Spin component 4.9		
		χ_{d0}	ω_d (MHz)	β	χ_{s0}	ω_s (MHz)	α
Mn–Zn ferrite	4.9	3282	2.5	9.3×10^6	1438	6.3	1.28
Ni–Zn ferrite	5.2	485	2.8	3.5×10^6	1130	1100	161

Table 2
Sample information of NiZnCu ferrite and NiZnCu ferrite composite reported by Kawano et al. [14]

Sample name	Weight ratio of NiZnCu ferrite (wt%)	Weight ratio of $Bi_2O_2+SiO_2$ (wt%)	Sintering time (h)	Density (g/cm^3)	Ferrite grain size (μm)
Sample A	100	0	6	5.16	≅12.67
Sample B-1	70	30	6	5.04	≅3.69

Table 3
Sample information of Ni_2Y ferrite and Ni_2Y ferrite composite reported by Shin and Oh [15]

Sample name	Weight ratio of Ni_2Y ferrite (wt%)	Weight ratio of silicon rubber (wt%)	Sintering time (h)
Sample Ni_2Y	100	0	3
Sample Ni_2Y composite	57	43	3

The complex magnetic permeability function $\mu(\omega)$ must be analytical in the area enclosed by the curve C (Fig. 1), their poles must be located in the complex superior semi-plane: this is one important property to verify the principle of causality and temporary independence.

2. Experimental

The loss factor of the complex magnetic permeability of sintered Mn–Zn, Ni–Zn, Ni_2Y, Ni_2Y and NiZnCu ferrites and their composites have been computed numerically applying the Hilbert transform to the real part of the ferrites, by using the results reported by Tsutaoka [6], Kawano et al. [14], and Shin and Oh [15] (See Tables 1–3). Those complex magnetic permeability responses were depicted and have been compared with the imaginary part of $\mu(\omega)$ computed numerically by means of the Hilbert transform obtained in this paper.

3. Results and discussions

According to the preceding discussion, the magnetic permeability complex function $\mu(\omega)$ must be analytical in the complex upper half-plane [10]. The magnetic circuit model [4] of the magnetic permeability (12) is analytic except at the poles (the zeros of the denominator), and the

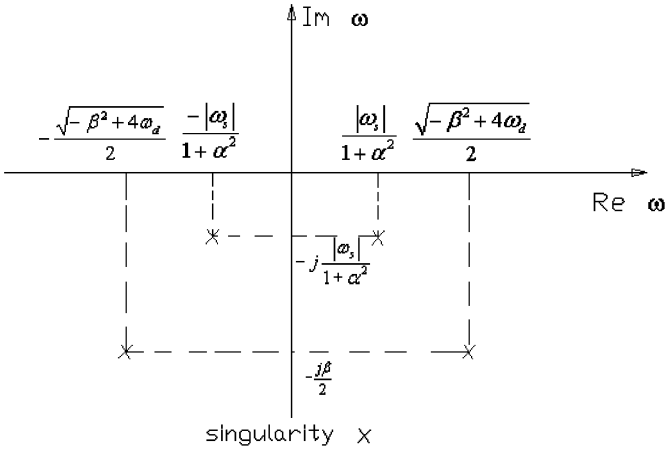

Fig. 2. Positions of the poles for the magnetic susceptibility.

expressions of that singular points are

$$\omega_{1,2} = \frac{-\mathrm{j}\beta \pm \sqrt{-\beta^2 + 4\omega_\mathrm{d}^2}}{2}, \tag{18}$$

$$\omega_{3,4} = \mathrm{j}\frac{-|\omega_\mathrm{s}|\alpha}{1+\alpha^2} \pm \frac{|\omega_\mathrm{s}|}{1+\alpha^2}. \tag{19}$$

The position of the poles from Eqs. (9) and (11) is illustrated in Fig. 2. $\omega_{1,2}$ are the poles that represent the movement of the domain's wall, while $\omega_{3,4}$ are the poles that represent the gyromagnetic spin rotation. It can be observed that all poles lay in the lower complex half-plane, as it belongs to a causal system [10,16].

The experimental data of μ' from Refs. [6,14,15] have been employed to calculate μ'' using the Hilbert transform as follows:

$$\mu'' = H_\mathrm{T}(\mu' - \mu'_{\mathrm{r}1}), \tag{20}$$

where H_T is the Hilbert transform.

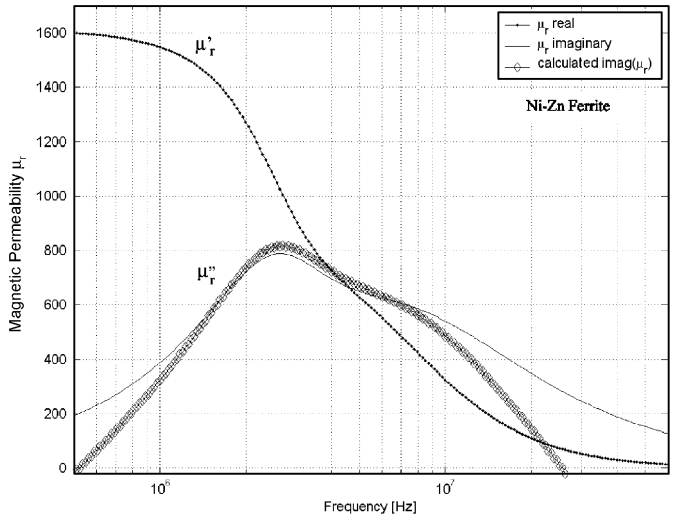

Fig. 3. Complex permeability spectra of sintered Ni–Zn ferrite.

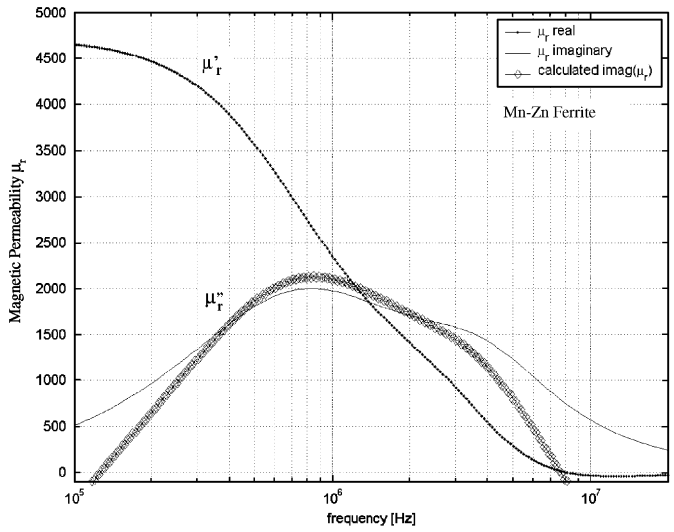

Fig. 4. Complex permeability spectra of sintered Mn–Zn ferrite.

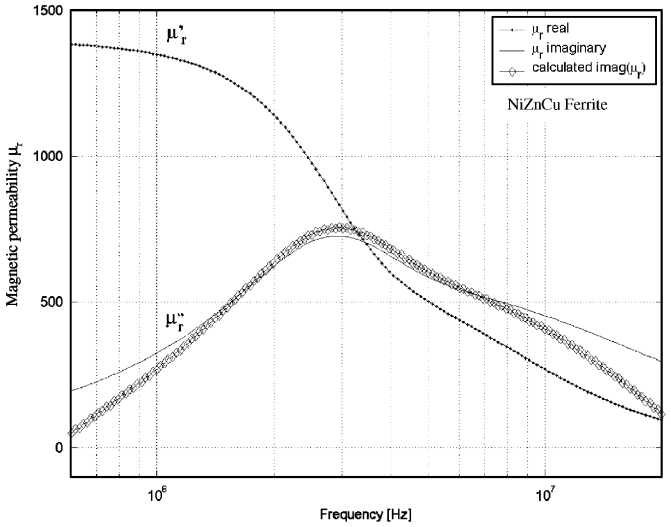

Fig. 5. Complex permeability spectra of NiZnCu ferrite (sample A).

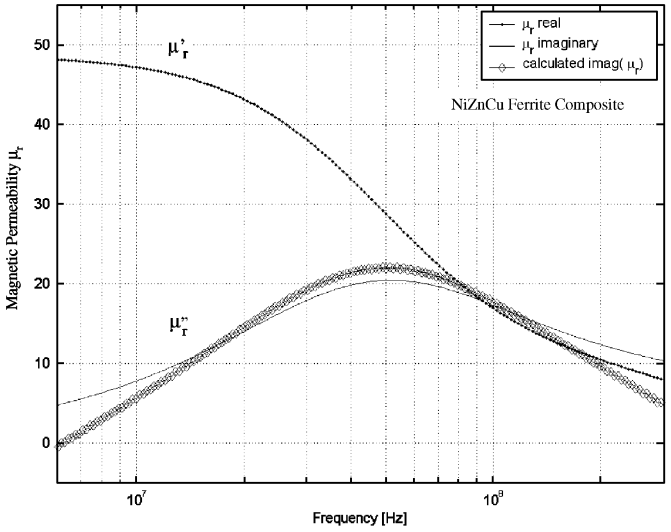

Fig. 6. Complex permeability spectra of Ni–ZnCu ferrite composite (sample B1).

Figs. 3–8 show the experimental results of μ' and μ'' taken from the reports and μ'' obtained numerically by mean of Hilbert transform in the present investigation. Experimental and calculated curves of magnetic loss spectra have fairly good coherence.

Fig. 3 shows the complex permeability spectra of the NiZn ferrite [6], where it can be observed that the calculated curve $\mu'' = H_T(\mu' - \mu'_{r1})$ fits with the experimental values in the central zone of the spectra, whereas it differs for frequencies smaller than 1 MHz and greater than 10 MHz. The loss peak of this ferrite is around 2.5 MHz, and a deformation can be observed, which is coherent with the calculated values for this frequency.

The complex permeability spectra of MnZn ferrite are shown in Fig. 4 [6]. The peak is located around 0.6 MHz; the calculated data are coherent with the experimental ones in the center of the spectra, whereas they differ in high and low frequencies.

In Fig. 5, the complex permeability spectra of the NiZnCu ferrite are shown. The frequency of the peak is located at 3 MHz and the calculated results match the measured results.

In Fig. 6, the complex permeability spectra of NiZnCu ferrite composite are shown. The loss peak is at 50 MHz and the coherence is as acceptable as in the previous ferrites.

In Fig. 7, the measurements and the numerical results of the Ni_2Y ferrite are depicted. Two peaks can be observed at 0.9 and 6.5 GHz; the calculated curve fits to the measured values along almost all the range of frequencies. It can be seen that when enlarging the rank of frequencies, the calculated results fit better to the experimental curve. In Fig. 8, the measurements and the numerical results of the Ni_2Y ferrite composite are depicted. The differences

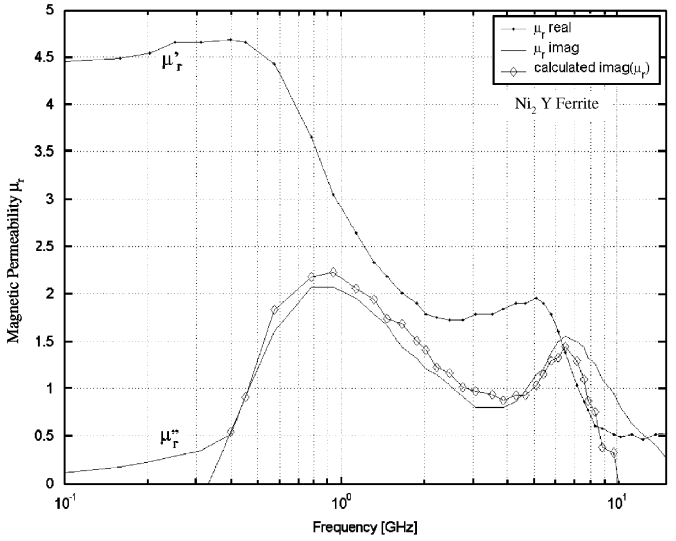

Fig. 7. Complex permeability spectra of Ni_2Y ferrite.

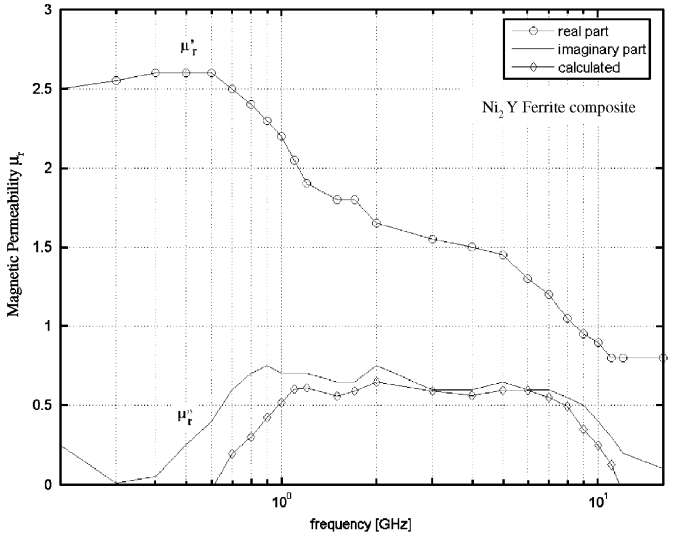

Fig. 8. Complex permeability spectra of Ni_2Y ferrite composite.

between both the curves can be observed specially at higher and lower frequencies. In almost all the graphs, it is observed that in maximum and minimum frequencies of the measured range, the error between the calculated and the measured losses increase, and an explanation will be provided here.

Theoretically, the bandwidth used to apply the Hilbert transform goes from $-\infty$ up to $+\infty$, as it has been expressed in Eqs. (15) and (16). This cannot be obviously reproduced in practice, but when the bandwidth is increased, the error in the numerical predictions of μ'' decreases.

4. Conclusion

The proposed model of the magnetic permeability as a function of the frequency for ferrites has been analyzed. This model fulfills the essential property of complex permeability spectra of ferrites: the absence of singular points in the superior semi-plane of the complex plane, which is a direct consequence of the physical principle of causality.

The magnetic loss factor of the NiZn, MnZn, Ni_2Y, and NiZnCu ferrites and their composites has been predicted successfully by mean of the computed Hilbert transform applied to the real part of the permeability.

From the above analysis, it can be concluded that this numerical technique can be applied to calculate the response of μ'', just by knowing μ'. This conclusion is important for experimental investigations in the complex permeability spectra of ferrites.

Acknowledgments

The authors thank to Facultad de Ingeniería, University of Buenos Aires, for the grant I017, and to the Comisión Nacional de Investigaciones Científicas y Tecnicas CONICET for the Grant PIP2355.

References

[1] J.A. Stratton, Electromagnetic Theory, McGraw-Hill Book Company, 1941.
[2] A. Von Hippel, Dielectrics and Waves, Wiley, 1954.
[3] R.F. Sohoo, Theory and Application of Ferrites, Prentice-Hall, Englewood Cliffs, NJ, USA, 1960.
[4] V. Trainotti, W.G. Fano, Ingeniería Electromagnética, Ed. Nueva Librería, Buenos Aires, Argentina, 2004.
[5] E.P. Wohlfarth (Ed.), Ferromagnetics Materials, vol. 2, North-Holland, Amsterdam, 1980 (Chapter 3).
[6] T. Tsutaoka, J. Appl. Phys. 93 (5) (2003) 2789.
[7] R.S. Trebble, D.J. Craik, Magnetic Materials, Wiley-Interscience, 1969, p. 605.
[8] W. Greiner, Classical Electrodynamics, Springer, 1998 (Chapter 16).
[9] R.V. Churchill, J.W. Brown, Complex Variables and Applications, McGraw-Hill, 1995.
[10] Landau y Lifchitz, Electrodinámica de los medios contínuos, Editorial Reverté, 1981.
[11] E.E. Sileo, R. Rotelo, S.E. Jacobo, Physica B 320 (2002) 257.
[12] A.C. Razzitte, W.G. Fano, S.E. Jacobo, Physica B 354 (2004) 228.
[13] A.C. Razzitte, S.E. Jacobo, W.G. Fano, J. Appl. Phys. 87 (9) (2000) 6232.
[14] K. Kawano, N. Sakurai, S. Kusumi, H. Kishi, J. Magn. Magn. Mater. 297 (2006) 26.
[15] J.Y. Shin, J.H. Oh, Trans. Magn. 29 (6) (1993) 3437.
[16] F. Greiner, Classical Electrodynamics, Springer, 1998 (Chapter 19).